DØ note 4586-CONF

Measurement of $\mathbf{B(t \to Wb)/B(t \to Wq)}$ at DØ

The DØ Collaboration
URL http://www-d0.fnal.gov

(Dated: August 26, 2004)

A measurement of the ratio of branching fractions, $R = B(t \to Wb)/B(t \to Wq)$, with q being any quark with $I_3 = -1/2$ and $Q = -1/3$, is presented. This analysis considers samples of single- and double-tagged lepton+jets events obtained with the DØ detector, corresponding to integrated luminosities of 169 pb^{-1} and 158 pb^{-1}, respectively in the e+jets and μ+jets channels. Two different lifetime taggers, CSIP and SVT, are used. The result found is:

$$CSIP: \ R = 0.65^{+0.34}_{-0.30}(stat)^{+0.17}_{-0.12}(syst)$$
$$SVT: \ R = 0.70^{+0.27}_{-0.24}(stat)^{+0.11}_{-0.10}(syst)$$

in agreement with the Standard Model expectation.

Preliminary Results for Summer 2004 Conferences

I. INTRODUCTION

In the framework of the Standard Model (SM), the ratio $R = B(t \to Wb)/B(t \to Wq)$ is constrained to be in the interval 0.9980-0.9984 at the 90% C.L. [1]. Within the SM, R can be expressed in terms of CKM matrix elements:

$$R = \frac{\mid V_{tb} \mid^2}{\mid V_{tb} \mid^2 + \mid V_{ts} \mid^2 + \mid V_{td} \mid^2} = \mid V_{tb} \mid^2 \tag{1}$$

The CKM matrix element $\mid V_{tb} \mid$ is indirectly constrained by the measurement of other CKM matrix elements, to the interval $0.9990 < \mid V_{tb} \mid < 0.9992$ at the 90% C.L. [1]. However the relation between R and $|V_{tb}|$ and the prediction for R are based on the assumption of the unitarity of the CKM matrix. The non-unitarity could for example arise from the existence of a fourth quark generation. The CDF collaboration has measured R using Run I data [2] and found it to be consistent with the SM prediction.

Experimentally, R can be determined by comparing the number of $t\bar{t}$ events with two identified b-jets in the final state with the number of events with one identified b-jet. In this scheme, one b-jet is used to identify a $t\bar{t}$ event, while another one allows to measure the relative fraction of $t \to Wb$.

This note reports the result of a measurement of $B(t \to Wb)/B(t \to Wq)$ based on the data collected by the DØ detector in Run II of Tevatron at a center of mass energy of $\sqrt{s} = 1.96$ TeV. The data samples correspond to an integrated luminosity of 169 pb^{-1} in e+jets and 158 pb^{-1} in μ+jets channels. The analysis is based on the background calculation and the tagging efficiencies determined in the $t\bar{t}$ cross section measurement using lifetime tagging [3] on the same data samples and considers events with exactly one or two identified b-jets.

II. DØ DETECTOR

The DØ Run II detector is comprised of the following main components: the central tracking system, the liquid-argon/uranium calorimeter, and the muon spectrometer.

The central tracking system includes a silicon microstrip tracker (SMT) and a central fiber tracker (CFT), both located in a 2 T superconducting solenoid magnet. The SMT is designed to provide efficient tracking and vertexing capability at pseudorapidities of $|\eta| < 3$. The system has a six-barrel longitudinal structure, each with a set of four layers arranged axially around the beampipe, and interspersed with 16 radial disks. A typical pitch of 50-80 μm of the SMT strips allows a precision determination of the three-dimensional track impact parameter with respect to the primary vertex which is the key component of the lifetime based b-jet tagging algorithms. The CFT has eight coaxial barrels, each supporting two doublets of overlapping scintillating fibers of 0.835 mm diameter, one doublet being parallel to the collision axis, and the other alternating by $\pm 3^o$ relative to the axis [4].

The calorimeter is divided into a central section (CC) providing coverage out to $|\eta| \approx 1$, and two end calorimeters (EC) extending coverage to $|\eta| \approx 4$ all housed in separate cryostats. Scintillators placed between the CC and EC provide sampling of showers at $1.1 < |\eta| < 1.4$ [5].

The muon system, covering pseudorapidities of $|\eta| < 2$, resides beyond the calorimetry, and consists of three layers of tracking detectors and scintillating trigger counters. Moving radially outwards, the first layer is placed before the 1.8 T toroid magnets, and the two following layers are located after the magnets [5].

III. EVENT PRESELECTION

While measuring R, we only consider top decays of the type $t\bar{t} \to WqWq$. One of the W bosons from top quark decay is required to decay leptonically (either prompt e or μ and neutrino or $e(\mu)$ from τ and corresponding neutrinos) and the other W boson is required to decay hadronically. These events have therefore the following signature: one high P_T isolated lepton, missing transverse energy from at least one undetected neutrino, two jets from hadronization of the down type quarks produced in the top decays and two jets from W boson decay. This will be referred to in the following as the ℓ+jets final state. Additional jets are often produced by initial or final state gluon radiation.

The event selection starts with the identification of W bosons decaying into a lepton and a neutrino. The signal samples for e+jets and μ+jets channels are preselected requiring, respectively, an electron ($E_T > 20$ GeV) candidate that satisfies tight quality identification criteria or an isolated muon ($P_T > 20$ GeV). The missing transverse energy must exceed 20 GeV in the e+jets channel and 17 GeV in the μ+jets channel.

The present analysis has a veto against a second high P_T lepton in order to remove Z production associated with jets. Nevertheless there is still a small acceptance for $t\bar{t}$ dilepton final states in which one lepton is not identified, falling outside the detector acceptance or below the identification selections.

To reduce contamination from events with missing transverse energy resulting from lepton energy mismeasurement, we require that the missing energy is not collinear with the lepton direction. The number of events containing a W produced in association with jets falls quickly at high jet multiplicity, while signal $t\bar{t}$ events are mostly concentrated in the third and fourth jet multiplicity bins. The first and the second jet bins, dominated by W production are used to cross check the background normalization.

IV. EVENT TAGGING PROBABILITIES FOR $t\bar{t}$ EVENTS

The procedure to calculate the event tagging probabilities in $t\bar{t}$ events where both top quarks decay to a W boson and a b-quark is described in Ref. [3]. The procedure is briefly summarized here while the emphasis is put on the way to compute the $t\bar{t}$ event tagging probablities in the case where R is different from one.

A. b-Tagging Efficiencies and Taggability

In order to decouple the tagging efficiency from detector related imperfections in the calorimeter or the tracking system the concept of "taggability" is introduced. Taggability is the probability for a jet to satisfy a certain criteria on the number of tracks and their momenta. It is determined on data and parameterised as function of the jet P_T and η.

The b-tagging efficiencies for both CSIP (Counting Signed Impact Parameter) and SVT (Secondary Vertex Tagger) are measured on a dijet data sample where b-jets decay semi-muonically. The efficiencies are then corrected to reproduce inclusive b-tagging efficiency using a Monte Carlo based correction factor. The probability to tag a light quark jet (mistag rate) is inferred from the negative tagging rate, while correcting for long lived particles inside light jets and for the effect of the heavy flavor content of the sample on the negative tag rate. The efficiency to tag a jet containing a c-quark is estimated based on the b-tagging efficiency in data and the Monte Carlo prediction for the b- to c-tagging efficiency ratio.

B. Event Tagging Probability for $R \neq 1$

While for a cross section measurement [3] the $t\bar{t}$ event tagging probabilities are calculated with the assumption that top quarks decay to Wb in 100% of the cases or R=1, this assumption is dropped in the present analysis. $t\bar{t}$ events can now be of three different types:

- $t\bar{t} \rightarrow W^+b\ W^-\bar{b}$ (further will be referred to as $tt \rightarrow bb$)
- $t\bar{t} \rightarrow W^+b\ W^-\bar{q}_\ell$ or its charge conjugate (referred to as $tt \rightarrow bq_\ell$)
- $t\bar{t} \rightarrow W^+q_\ell\ W^-\bar{q}_\ell$ (referred to as $tt \rightarrow q_\ell q_\ell$),

where q_ℓ denotes either a d- or a s-quark. The $t\bar{t}$ event tagging probabilities are computed separately for the three types of $t\bar{t}$ events mentioned above using the proper b-tagging and light jet tagging probabilities and are then combined to give the total $t\bar{t}$ tagging probability for a given value of R and for exactly 1 tag or 2 or more tags:

$$P_{\mathrm{n-tag}}(tt) = R^2 P_{\mathrm{n-tag}}(tt \rightarrow bb) + 2R(1-R)P_{\mathrm{n-tag}}(tt \rightarrow bq_\ell) + (1-R)^2 P_{\mathrm{n-tag}}(tt \rightarrow q_\ell q_\ell), \quad (2)$$

where R determines the fractions of the three types of $t\bar{t}$ events and n=1 or $\geq$2.

V. BACKGROUNDS

The backgrounds to $t\bar{t}$ events in the lepton+jets channel are QCD multijet production and W boson production in association with jets. Small additional background contributions arise from Z production with jets, dibosons, and single top production, which are estimated using Monte Carlo simulation. Further details on the background calculations can be found in Ref. [3].

The separation of the background where the lepton is not expected to pass the tight lepton criteria (QCD) from the other backgrounds (W+jets, diboson, single top and Z+jets) is achieved using the Matrix Method [6] which makes use of the different probability for a lepton from QCD and W- or Z-decay to pass a certain selection criteria. This

	3 jets		≥4 jets	
Before tagging	1105		295	
	CSIP	SVT	CSIP	SVT
=1 tag	74	68	44	43
Background	49.3±1.2	38.7±0.9	14.7±0.8	11.3±0.6
≥2 tags	7	8	8	6
Background	3.41±0.09	2.90±0.10	1.24±0.06	1.00±0.11

TABLE 1: Number of predicted background events and observed event yields.

Jet energy scale	0.034	-0.029
Top mass	0.002	-0.005
Taggability in data	0.001	-0.002
Semileptonic b-tagging efficiency in MC	0.029	-0.027
Semileptonic b-tagging efficiency in data	0.140	-0.096
NTRF parametrization	0.012	-0.012
b-decay model dependence	0.026	-0.026
QCD tagging probability	0.036	-0.036
Wbb, W(bb), Wcc, W(cc) cross sections	0.018	-0.017
Event statistics for Matrix Method	0.017	-0.019
Total systematic	0.171	-0.119

TABLE 2: The main systematic errors on R in the combined ℓ+jets channel for CSIP.

can be done either before applying b-tagging (in the case of e+jets analysis) or after tagging the data (in the case of μ+jets analysis). The QCD contribution to the tagged e+jets data was estimated as the product of the number of QCD events in the preselected sample times the probability to tag a QCD event measured directly on data. The number of tagged W+jets events is derived based on the number of W+jets events observed in the data before tagging, multiplied by the tagging probability for W+jets events. The event tagging probability for W+jets is derived from the fractions of the various jet flavor combinations associated to the W production and the probabilities to tag each combination.

Table 1 summarizes the number of observed ℓ+jets events before and after tagging by both taggers together with the expected number of background events. The difference between the number of observed tagged events and the predicted background is considered to be the $t\bar{t}$ contribution consisting of $tt \to bb$, $tt \to bq_\ell$ and $tt \to q_\ell q_\ell$ final states.

VI. LIKELIHOOD MAXIMIZATION PROCEDURE

The value of R is calculated for CSIP and SVT separately by performing a maximum likelihood fit of R and the top production cross section to the observed number of tagged events. Each analysis is considered as 8 different channels (electron or muon, 3 or ≥4 jets and 1 or ≥2 tags). If the index j runs over e+3 jets, e+4 jets, μ+3 jets, μ+4 jets then the likelihood $\mathcal{L}(N_j^{\rm obs}|R,\sigma_{t\bar{t}})$ to observe the set of tagged events in data is proportional to:

$$\prod_{j=1}^{4}\mathcal{P}(N^{\rm obs}_{j,1\ tag},N^{\rm predicted}_{j,1\ tag})\prod_{j=1}^{4}\mathcal{P}(N^{\rm obs}_{j,2\ tags},N^{\rm predicted}_{j,2\ tags}) \quad (3)$$

where $N^{\rm obs}_{j,n\ tag}$ is the number of observed events in channel j with n tags and $N^{\rm predicted}_{j,n\ tag}$ is the prediction in the same channel. The predicted number of events are functions of R and the $t\bar{t}$ cross section. Here $\mathcal{P}(N^{\rm obs};N^{\rm predicted})$ denotes the Poisson probability to observe $N^{\rm obs}$ events when the prediction is $N^{\rm predicted}$.

In order to take into account the Poisson statistics of the number of events entering the Matrix Method in the e+jets and μ+jets channels additional Poisson terms are introduced while accounting for correlations between event populations.

The systematic uncertainties on R are obtained for each independent source of uncertainty by varying the source by one standard deviation up and down and propagate the variation into both background estimates and signal efficiencies. A new likelihood function is constructed for each variation to derive a new optimal R and cross section. These deviations from the central value of R are then added in quadrature to obtain the total systematic uncertainty.

Jet energy scale	0.022 -0.032
Top mass	0.006 -0.007
Taggability in data	0.002 -0.003
Semileptonic b-tagging efficiency in MC	0.034 -0.039
Semileptonic b-tagging efficiency in data	0.079 -0.071
NTRF parametrization	0.004 -0.005
b-decay model dependence	0.028 -0.026
QCD tagging probability	0.039 -0.039
Wbb, W(bb), Wcc, W(cc) cross sections	0.020 -0.019
Event statistics for Matrix Method	0.010 -0.010
Total systematic	0.106 -0.103

TABLE 3: The main systematic errors on R in the combined ℓ+jets channel for SVT.

VII. RESULTS

The value of R is calculated separately for the CSIP and SVT taggers. The results below give the fitted value of R when R and the $t\bar{t}$ cross section are fitted simultaneously. The corresponding negative log-likelihood curves are shown in Figures 1 and 2. The results are:

$$CSIP: \ R = 0.65^{+0.34}_{-0.30}(stat)^{+0.17}_{-0.12}(syst)$$
$$SVT: \ R = 0.70^{+0.27}_{-0.24}(stat)^{+0.11}_{-0.10}(syst)$$

consistent with the Standard Model prediction. The 68% and 90% C.L. contours in the $\sigma_{t\bar{t}}$ versus R plane are shown for CSIP and SVT in Figures 3 and 4.

A summary of the major systematic uncertainties taken into account in the present analysis are shown in Tables 2 and 3. While the result above is obtained by fitting the $t\bar{t}$ cross section and R simultaneously the value of R can be fixed and the cross section derived for different values of R. The fitted value of the $t\bar{t}$ cross section for a given fixed value of R is given as a function of R for both CSIP and SVT in Figures 5 and 6. The size of the statistical error on the $t\bar{t}$ cross section when R is know with infinite precision is given by the shaded area.

Acknowledgments

We thank the staff at Fermilab and collaborating institutions, and acknowledge support from the Department of Energy and National Science Foundation (USA), Commissariat à L'Energie Atomique and CNRS/Institut National de Physique Nucléaire et de Physique des Particules (France), Ministry for Science and Technology and Ministry for Atomic Energy (Russia), CAPES, CNPq and FAPERJ (Brazil), Departments of Atomic Energy and Science and Education (India), Colciencias (Colombia), CONACyT (Mexico), Ministry of Education and KOSEF (Korea), CONICET and UBACyT (Argentina), The Foundation for Fundamental Research on Matter (The Netherlands), PPARC (United Kingdom), Ministry of Education (Czech Republic), Natural Sciences and Engineering Research Council and WestGrid Project (Canada), BMBF (Germany), A.P. Sloan Foundation, Civilian Research and Development Foundation, Research Corporation, Texas Advanced Research Program, and the Alexander von Humboldt Foundation.

[1] S. Eidelman et al., Phys. Lett., B592, 1 (2004).
[2] CDF Collaboration, T. Affolder *et al.*, Phys. Rev. Lett. **86**, 3233 (2001).
[3] DØ Collaboration, conference note 4565-conf available at http://www-d0.fnal.gov/Run2Physics/WWW/results/TOP/T05/T05.pdf
[4] V. Abazov et al. (DØ Collaboration), in preparation for submission to Nucl. Instrum. Methods Phys. Res. A;
T. LeCompte and H.T. Diehl, "The CDF and DØ Upgrades for Run II", Ann. Rev. Nucl. Part. Sci. **50**, 71 (2000)
[5] S. Abachi et al. (DØ Collaboration), Nucl. Instrum. Methods Phys. Res. A **338**, 185 (1994).
[6] DØ Collaboration, S. Abachi *et al.*, FERMILAB-Conf-03/200-E.

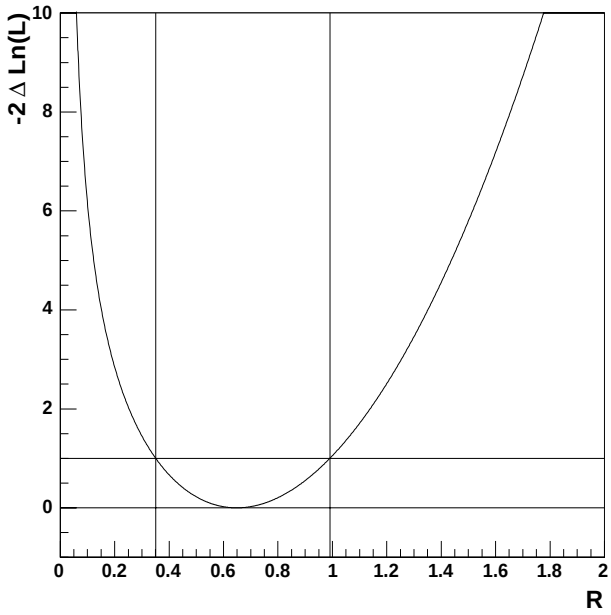

FIG. 1: *The negative log likelihood versus R for the combination of e+jets and μ+jets channel for CSIP.*

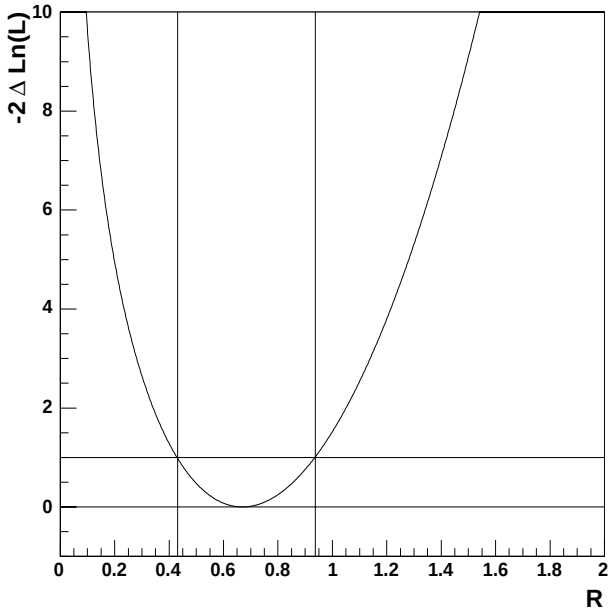

FIG. 2: *The negative log likelihood versus R for the combination of e+jets and μ+jets channel for SVT.*

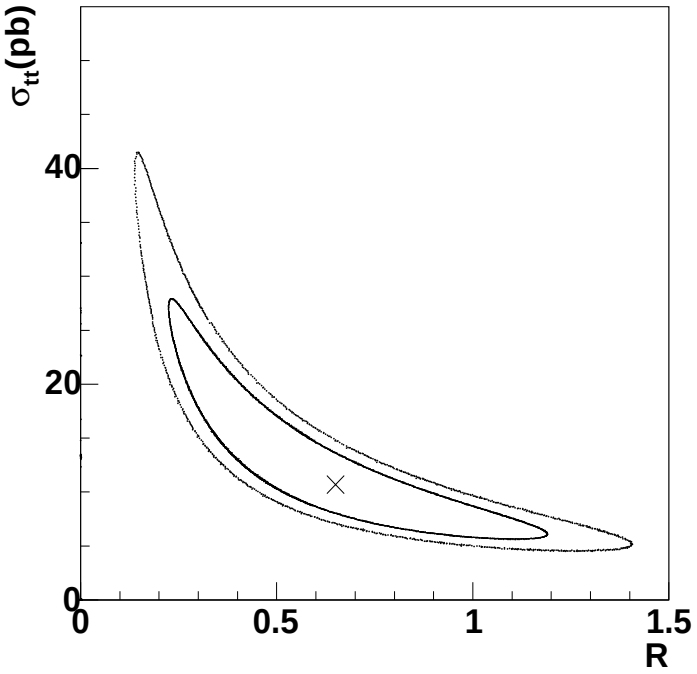

FIG. 3: *The 68% and 90% C.L. contours in the plane defined by the $t\bar{t}$ cross section and R for e+ jets and μ+ jets combined with the CSIP tagger. The maximum of the likelihood is shown by the star.*

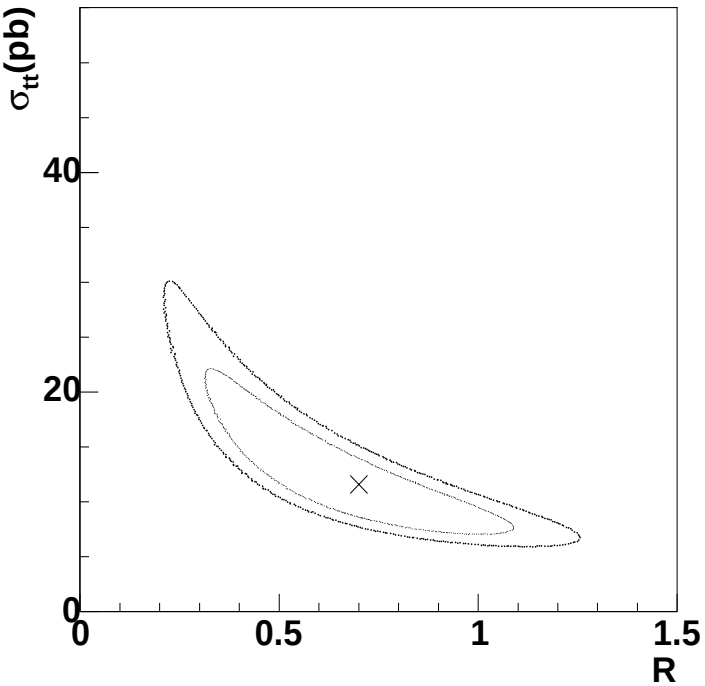

FIG. 4: *The 68% and 90% C.L. contours in the plane defined by the $t\bar{t}$ cross section and R for e+ jets and μ+ jets combined with the SVT tagger. The maximum of the likelihood is shown by the star.*

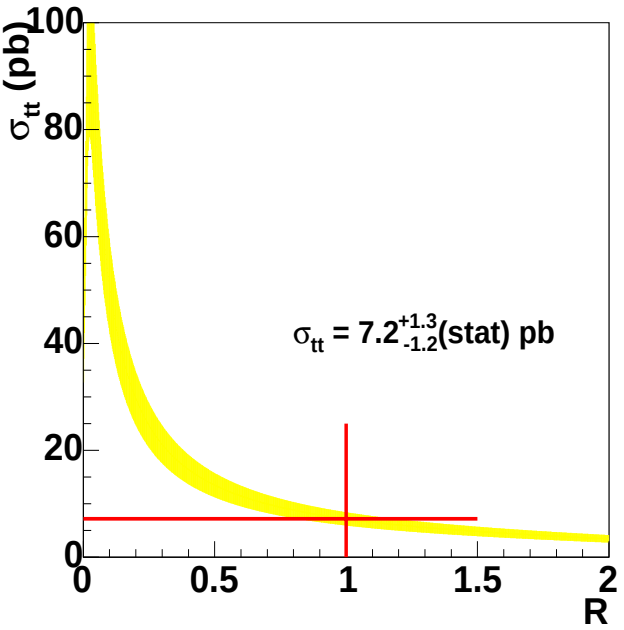

FIG. 5: *The fitted $t\bar{t}$ cross section when the value of R is fixed as function of R, here shown for CSIP in the e+jets and μ+jets channels combined. The shaded area represents the statistical uncertainty on the cross section when R is known with infinite precision. The straight lines and the given $t\bar{t}$ cross section show the resulting cross section when R is fixed to unity.*

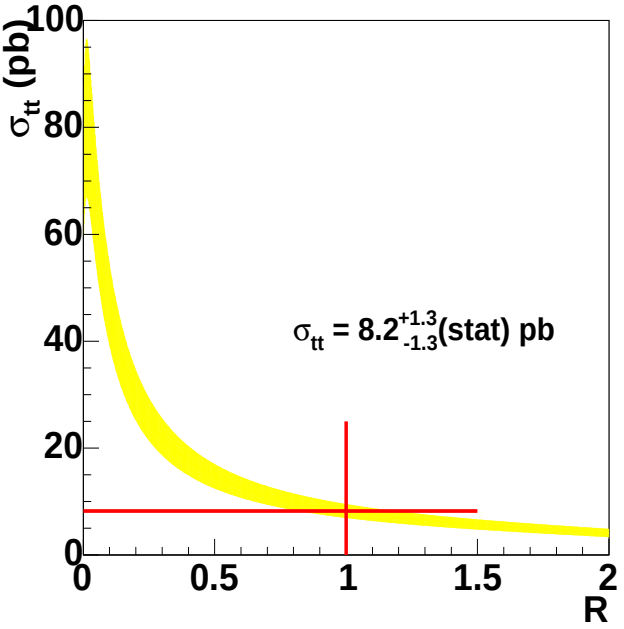

FIG. 6: *The fitted $t\bar{t}$ cross section when the value of R is fixed as function of R, here shown for SVT in the e+jets and μ+jets channels combined. The shaded area represents the statistical uncertainty on the cross section when R is known with infinite precision. The straight lines and the given $t\bar{t}$ cross section show the resulting cross section when R is fixed to unity.*